Sensor Optimization Using a Genetic Algorithm for Structural Health Monitoring in Harsh Environments

Ying Huang[1*], Simone A. Ludwig[2], and Fodan Deng[1]

[1]Department of Civil and Environmental Engineering, North Dakota State University

1340 Administration Ave., Fargo, ND 58108, USA

[2]Department of Computer Science, North Dakota State University

1340 Administration Ave., Fargo, ND 58108, USA

* *Corresponding author: ying.huang@ndsu.edu; Tel: 701-231-7651; Fax: 701-231-6185.*

Abstract Structural health monitoring (SHM) has become a powerful tool for engineering fields to make decisions for resource allocation in harsh environments such as fire, earthquake, flood, etc. To effectively make a decision based on the monitoring data, the SHM system requires a large number of sensors for different data resource measurements, for example, strain, temperature, and vibration, resulting in a need to determine the tradeoff between the number of sensors of each type and the associated cost of the system. This paper introduces a sensor optimization approach based on genetic algorithm for the multiple-objective sensor placement of structural health monitoring in harsh environments. The derived theoretic multi-task objective function of the genetic function is validated by a single-bay steel frame in a harsh environment of simultaneous high temperature and large strain. The variance between the theoretical and the experimental analysis was within 5%, indicating an effective sensor placement optimization using the developed genetic algorithm, which can be further applied to general sensor optimization for SHM system applications in harsh environments.

Keywords: Sensor Optimization, Structural Health Monitoring, Genetic Algorithm, Harsh environment

1. Introduction

A structural health monitoring (SHM) system has recently gained exceeding attention from engineering fields and it has been successfully applied to various civil infrastructures such as tall buildings, long bridges, hospitals, offshore facilities, nuclear power plants, etc. By collecting specific data from sensors on structures, the health condition of the structures can be analyzed in real time, which could help the users to track the structural damages, allowing associated maintenance in advance, and thus avoid severe fatality. However, compared with large-scale civil infrastructure, the lightweight sensors in an SHM system would be more vulnerable for damages, especially in harsh environments.

A harsh environment describes a structural surrounding with potential high temperature involvement such as fire, appearance of reactive chemical substance and radiations such as corrosive environments, or an attack of high pressure or vibration such as an earthquake. Harsh environments may fail the allowable working condition of a sensor, leading to a sensor failure. When the number of failed sensors exceed an acceptable level, the SHM system would produce an unreliable monitoring or prediction of the structural performance. To avoid the occurrence of such condition, current practice uses high-cost harsh-environment resistant sensors with extensive redundancies of sensor placement for an SHM system in harsh environments, resulting in a high-cost and unaffordable system to be widely applied.

Therefore, to search for an affordable SHM system in harsh environments, it needs to reduce the total numbers of sensors while remaining an acceptable monitoring accuracy at the same time, requiring a sensor placement optimization for sensor location, sensor types and number (cost), and measurement accuracy. Sensor optimization problem, despite static or dynamic, is incorporated in a special class of mathematic problems, a convex optimization, which has been discussed for almost 100 years [1]. Unfortunately, the sensor selection problems have been proved to be NP-hard, which could result in a long execution time depending on the problem size. In order to get an exact solution, even with a powerful computer, the number of sensor candidates has to be reasonably small [2, 3]. In last two decades, new developments in this mathematic area brought us further possibilities to get the solution of sensor optimization problems more effectively and efficiently [4].

Instead of an exact solution, recent approaches for sensor optimization focus on solving the problem approximately using local search methods. For the control and damage detection of dynamic structures, either local information-theory-based [5-11] or information-based [12-15] sensor placement optimizations can be applied. These local search methods frequently form the optimizing control function of the fisher information matrix (FIM) or its variants using structural dynamic properties, such as structural frequency mode shapes, strain energy, and structural curvature. Thus, these optimization methods emphasize either the controllability or observability of the system and are usually applied for placement of wireless acceleration sensors on structures. In addition, the computational performance of these local search approaches are suboptimal and not guaranteed to be minimum since these algorithms reduce the sensor number in an iterative manner.

Global search methods have also been investigated such as Genetic algorithm (GA) [16, 17] and swarm intelligence method [18]. The GA was developed by Alan Turing as "learning machine" in 1950 and started to become popular in the late 1980s due to the computational ability of desktop computers [19]. The GA has great advantages for multi-dimensional, non-differential, and non-continuous problems since it does not rely on an error surface and can be easily transferred from one model to another. Being a global search method, the GA has been widely used in sensor placement optimization problems for SHM systems such as active vibration control [16, 17, 20]. However, traditional GAs can be inefficient because they show a tendency of early convergence, and poorly known fitness functions that generate bad chromosomes causing in a failure of solving the sensor selection problems [19]. There are several modified GA applications of the sensor optimization [21-26]. Recent research combined multiple algorithms to achieve optimization for the sensor placement [27-29].

In addition, various intelligent algorithms have also been developed as good tools for wireless sensor placement in a regular environment with consideration to optimize power consumption and signal strength, such as the monkey algorithm and glowworm swarm optimization algorithms [30-32]. However, in harsh environments, multiple sensor types will be involved such as strain sensors, temperature sensors, and vibration sensors, and the major task of optimization is to determine the optimized number of each sensor type. None of these applications consider more than one type of sensor for SHM application in harsh environments, and thus, this is the contribution of this paper.

In this paper, we introduce a new approach based on GA to solve the sensor selection problem for SHM application in harsh environments where multiple types of sensors is a necessity. GA was chosen since it is a very well understood optimization algorithm with few parameters that need to be determined in advance. Furthermore, the authors have experience with GA, and thus, have chosen the GA to be applied to the sensor optimization problem. The developed algorithm uses a fitness function with consideration of the tradeoff between the sensor number/type and the measurement accuracy with a weight factor, which can better serve as decision-making criteria. The organization of the remaining paper is as follows: Section 2 introduces the developed GA, which can be used for sensor optimization of general SHM systems in harsh environments. Section 3 conducts a sensitivity study of the sensor deployment using a single-bay steel frame structure as a case study. Section 4 validates the reliability of the developed method using laboratory experiments. Finally, Section 5 provides the conclusion and outlines the potential future work.

2. Genetic Algorithm based Sensor Placement Optimization Approach

This section introduces the GA based sensor placement optimization method used to find the optimal number of sensors of a SHM system in harsh environments applied to different placement configurations of multiple sensor types. The optimization method referred to as genetic algorithm belongs to the family of evolutionary algorithms, which are inspired by natural phenomena of biological evolution. An evolutionary algorithm uses natural selection (biologically referred to as survival of the fittest) to improve the fitness of the overall population, when a population of individuals is given. With a function to be maximized, a set of candidate solutions is randomly created and the fitness function used as a fitness measure (the higher the better) is applied. Based on this fitness measure, some of the better candidates are chosen to undergo recombination and mutation. Recombination is applied to two candidates and results in one or more new candidates, whereas mutation is only applied to one candidate and results in one new candidate. After recombination and mutation are applied, a set of new candidates replaces the old ones and the next generation begins. This process repeats until a candidate with sufficient quality shows up or a predefined number of iterations is reached [33].

Fig. 1 shows the overview diagram of a general GA-based sensor placement optimization. First, the problem needs to be encoded using the chromosome representation, and the fitness equation needs to be defined. Afterwards, the selection method needs to be chosen, and the crossover and mutation operations need to be defined. Given that the sensor placement problem is a combinatorial optimization problem, the operators such as crossover and mutation that apply for continuous problems do not apply for combinatorial problems and thus need to be redefined.

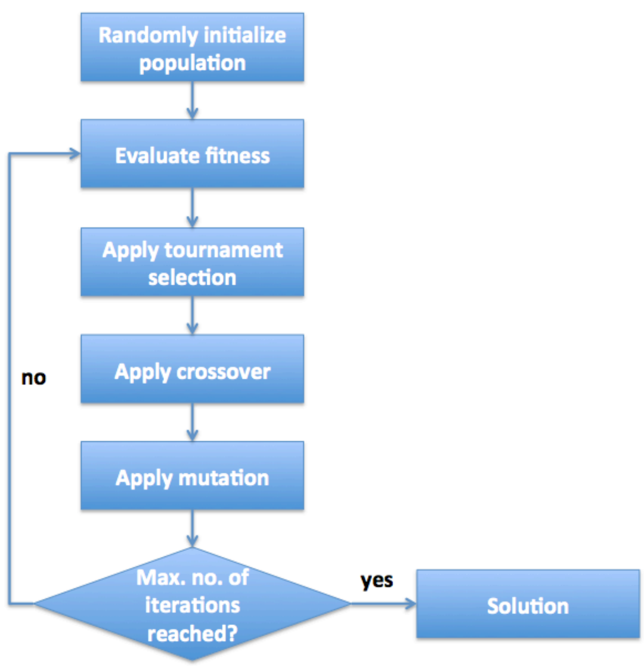

Fig. 1 Flowchart of a general GA algorithm

The overall flow of the algorithm is as follows: first, a randomly generated population is initialized, then the fitness of each chromosome (solution) is evaluated, afterwards the selection process is run whereby the tournament selection method was chosen. Then, crossover and mutation operations are applied in order to recombine potentially better solutions. The algorithm terminates once the maximum number of iterations has been achieved, and the solution is obtained representing the optimized sensor placement.

Chromosome encoding: The chromosome will have a structure as follows. The position of the sensors is encoded based on the position within the chromosome whereas the location with only one type of sensor is denoted by a 1, with two types of sensors being present at a particular location this is denoted by a 2, and correspondingly, the location with N types of sensors is denoted by N.

Fitness equation: The optimization in this study is to minimize the measurement error, resulting in the maximization of the measurement accuracy. At the same time, the optimization minimizes the measurement cost by analyzing the trade-off between measurement accuracy and cost. Figure 2 shows the flowchart of the developed GA algorithm with consideration of the specific fitness equation. The fitness equation for the sensor placement optimization is given as:

$$\sum A = \min \sum f\left[F_{1,i}(x_i, y_i, z_i), F_{2,i}(x_i, y_i, z_i), \cdots, F_{N,i}(x_i, y_i, z_i)\right] \tag{1}$$

where i is the time; (x_i, y_i, z_i): x_i is the x^{th} coordinate at time i; y_i is the y^{th} coordinate at time i; $z_{i,}$ is the z^{th} coordinate at time i. $F_{N,i}$ is the measurement from the type-N sensor at time i and $f(\ldots)$ is the optimization function that consists of two parts as:

$$f(i,j) = \max[w \cdot a_N(i,j) + (1-w) \cdot c_N(j)] \tag{2}$$

where w is the weight factor, a is the accuracy function and c is the cost function, respectively. j is the sensor location identification number, the sum of j will be the maximum number of sensors, n.

The accuracy function, $a_N(i,j)$, is defined as $1 - e_N(i,j)$, where $e_N(i,j)$ is the error function stated as follows:

$$a_N(i,j) = 1 - e_N(i,j) = 1 - \sqrt{\left(\frac{F_{1,actual,i} - F_{1,i}(j)}{F_{1,actual,i}}\right)^2 + \cdots + (\frac{F_{N,actual,i} - F_{N,i}(j)}{F_{N,actual,i}})^2} \quad (3)$$

Thus, if an error function is 1, the accuracy function will be 0 and if the error function is 0, then the accuracy function will become 1. $F_{N,i}(j)$ is the linear interpolating value between the measurement of two nearby sensors at the same location given as $F_{N,\text{actual},i}$, j is the sensor identification number which can be described as the data set location, sum of j equals to the total data set. The linear interpolating values of $F_{N,i}(j)$ is given as:

$$F_{N,i}(j) = F_N(j) + \frac{F_N(j) - F_N(j+1)}{L} x_i \quad (4)$$

where, $F_{N,i}(j)$ is the measured data from type-N sensor at location j from the sensor measurements, $F_N(j+1)$ is the measured data from type-N sensor at location $j+1$, L is the distance between the sensor j and $j+1$, x_i is the distance between sensor location j and the calculation time i.

The second part of the optimization function is the cost function, which is evaluated as follows:

$$c_N(j) = \frac{1}{\sum_1^N (\sum j \cdot b_N)} \quad (5)$$

where $\sum j$ is the sum of the type-N sensors based on the sensor location j, and b_N is the unit price of the type-N sensor. Thus, the maximum $c_N(j)$ is 1 when no sensors are placed, and the minimum $c_N(j)$ is 0 when all the locations have sensors.

Selection method and crossover operation: The tournament selection method [34] was chosen as the selection method. The selection method, in general, enables better or fitter chromosomes (solutions) to be chosen more frequently compared to less fit chromosomes. The tournament selection method works as follows. Several "tournaments" are run between the individuals that are chosen at random from the population, and the winner of each tournament is then used for the crossover operation.

The crossover operation takes two chromosomes and assures that the crossover point of each chromosome is in the middle such that an equal amount of sensors are on either side of the crossover breakpoint. This allows the different crossover pairs to be connected together without the need of chromosome repair afterwards.

Mutation operation: The mutation operation works on a single chromosome whereby two genes within the chromosome are chosen at random and exchanged accordingly. This also ensures that the number of sensors will remain the same after the mutation has been applied. The termination criterion is the maximum number of iterations specified, i.e., the genetic algorithm will stop once the maximum number of iterations has been reached.

Preliminary experiments were used to establish the best parameters (population size, crossover probability, mutation probability) to use for the GA run. Each data point shown in the following figures (Fig. 3 and 5) is the average of 25 independent runs of the GA algorithm. A population size of 500 was determined after running preliminary experiments for population sizes of 400, 500, and 600. The fitness values obtained were 0.843512, 0.844315, and 0.843498, respectively. As for the crossover probability, crossover values of 0.6, 0.7, and 0.8 achieved fitness values of 0.844031, 0.844315, and 0.844312, respectively. Thus, a crossover probability of 0.7 was chosen. Similar runs were performed with varying mutation probabilities of 0.05, 0.1, and 0.15 achieving fitness values of 0.843527, 0.843153, and 0.843691, respectively. Thus, the mutation probability was set to 0.1. As for the maximum number of iterations, a value of 5,000 was chosen after observing the convergence graph ensuring that convergence has occurred.

3. Sensitivity Study

The objective function in Section 2 indicated that a tradeoff exists between the measurement accuracy and system cost for the sensor placements when performing SHM in harsh environments. Three factors will influence this tradeoff significantly including the total number of sensors, sensor type, and sensor locations. With given sensor types and criteria for the required measurement accuracy, the developed GA will search for the optimized total number of sensors and its corresponding sensor locations. This section conducts the sensitivity study of the developed GA approach on sensor placement optimization for structural health monitoring using a case study of a single-bay steel frame in a fire environment.

3.1 Generation of Training Set Using Finite Element Modeling

To generate the training set for the sensitivity study of the developed GA for sensor optimization of SHM system in harsh environments, a finite element (FE) model of a single-bay steel frame was built and analyzed using commercial FE program, ABAQUS [35]. Fig. 3(a) shows the 3-D FE model of the single-bay steel frame made up by two columns (height: 84 in. or 2.13m) and one top beam (length: 56 in. or 1.42m). The columns of the steel frame were modeled to be hot-rolled A36 steel S3×5.7, which has a flange width of 3 inches (7.62cm) and a height of 4 inches (10.16cm). Hot-rolled A36 steel S5×10 was used for the top beam of the steel frame to meet the requirement of at least 5 times larger stiffness than the column. To ensure a rigid beam-column connection, stiffened beam-column connections were used in the FE model. Between various structural components, perfect ties connections were applied.

To a more accurate structural assessment in harsh environments, multiple structural health indicators were considered in this case study by simulating the steel frame under a fire environment. The assessment of the structural health condition of this steel frame, thus, can be evaluated based on two significant parameters: the strain and temperature distribution. The fire environment was modeled by changing the temperature distribution gradually on the middle of the left column from room temperature (72 °F) to 700 °C (1,292 °F), following reference [35]. The material properties of the steel frame as a function of temperature follows reference [35]. Coupled temperature-displacement trilinear element (C3D8T, C3D6T, and C3D4T in ABAQUS) was used for the FE analysis. The C3D8T is an 8-node thermally coupled brick, trilinear displacement and temperature [36]. The mesh ended a total of 8,750 elements as also shown in Fig. 3(a). The bottom ends of the two columns of the steel frame were fixed to the ground and mechanical loading was applied in the middle of the top beam of 254 lb/in^2 (175 N/cm^2) for an area of 6 in. ×6 in. (15.24cm × 15.24cm).

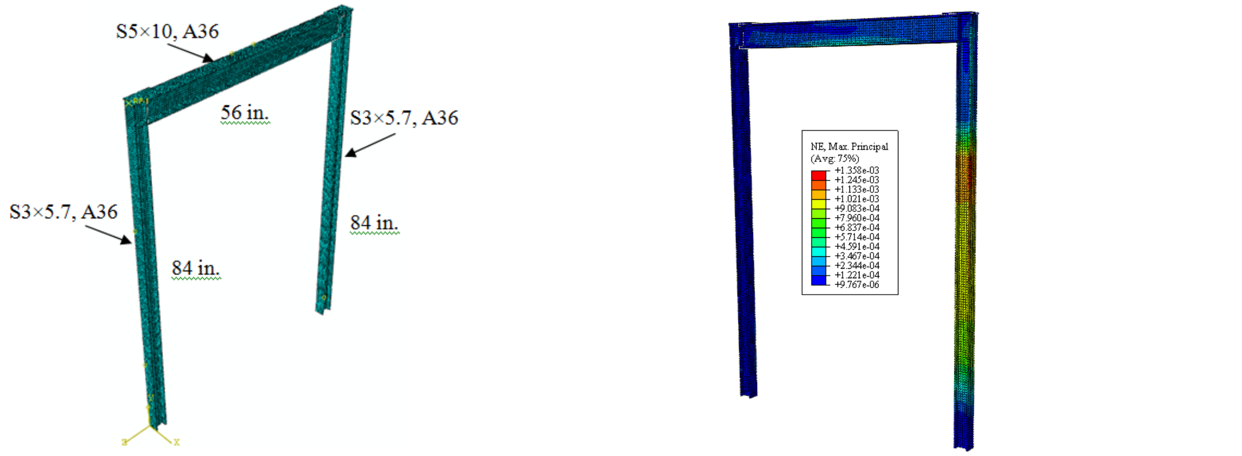

(a) The setup of FEM model (b) Strain distribution at temperature environment 212℉ (100°C)

Fig. 2 FEM model and the simulated strain distribution at fire temperature of 212 °F (100 °C)

Fig. 2(b) shows the strain distribution with fire temperature at 212 °F (100 °C). With most of the strain and temperature changes concentrated on the left column with fire loads, sensor placement optimization only was considered on this column. The simulated strain and temperature distribution data from the bottom to top of the column was used to feed into the developed algorithm for training purposes. A total of 84 nodes were identified for potential sensor placement with one inch (2.54cm) apart from one to another. Thus, a total 84 data points (maximum sensor locations) was used to train the developed algorithm with various temperature environments.

3.2 Generation of GA Fitness Function

In this case study, two types of sensors were considered, including temperature and strain sensors. Thus, the function of measurement accuracy in this case study can be specifically obtained as follows:

$$a(i,n,m) = 1 - \sqrt{\left(\frac{T_{actual,i}-T_i(n)}{T_{actual,i}}\right)^2 + \left(\frac{\varepsilon_{actual,i}-\varepsilon_i(m)}{\varepsilon_{actual,i}}\right)^2} \qquad (6)$$

in which, $T_i(n)$ and $\varepsilon_i(m)$ are the linear interpolating value between the temperature and strain measurement of two nearby sensors at the same location given as T_{actual} and $\varepsilon_{\text{actual}}$. At the two ends of the interested subject, room temperature and zero strain are assumed as boundary conditions. *n* and *m* are the location of the each type of sensor and the sum of n and m will be the number of each type of sensor, respectively. The linear interpolating values of $T_i(n)$ and $\varepsilon_i(m)$ are given as:

$$T_i(n) = T(n) + \frac{T(n)-T(n+1)}{L} x_i \quad \text{and} \quad \varepsilon_i(m) = \varepsilon(m) + \frac{\varepsilon(m)-\varepsilon(m+1)}{L} x_i \tag{7}$$

where, $T_i(n)$ is the temperature data at location i from sensor measurements, $T(n)$ is the temperature at sensor location n, and $T(n+1)$ is the temperature at sensor location n+1, L is the distance between the sensor n and n+1, x_i is the distance between sensor n location and the calculation location i. The same principle applies to the strain equation $\varepsilon_i(m)$.

The cost function, thus, can be simplified to:

$$c(n, m) = \frac{1}{(\sum n) \cdot b + (\sum m) \cdot cm} \tag{8}$$

where $\sum n$ is the sum of the temperature sensors based on the sensor location n, and $\sum m$ is the sum of the strain sensors based on the strain sensor locations, b is the unit price of the temperature sensors, and c_m is the unit price of the strain sensors.

Therefore, the fitness function in Eq. (3) can be specifically simplified as:

$$\sum A = \min \sum f[T_i(x_i, y_i, z_i), \varepsilon_i(x_i, y_i, z_i)] \tag{9}$$

where $f(i, j) = \max\,[w \cdot a(i, n, m) + (1 - w) \cdot c(n, m)]$.

With the defined fitness function, the data training for the sensitivity study was performed following the procedure described in Section 2 on the total number of sensors (n+m) and sensor type N. For the GA implementation, the population size was set to 500, the tournament size was 2, the crossover and mutation probabilities were 70% and 10%, respectively, and the maximum number of iterations was set to 5,000.

3.3 Sensitivity on Total Numbers of Sensors

To analyze the sensitivity of the GA on the total number of sensors, an analysis was performed by changing the total number of strain sensors from 3 until 84 with increments of 3 at four different temperature environments from 212 °F (100 °C) to 1,292 °F (700 °C). It is assumed that at each strain sensor location, one corresponding temperature sensor was placed. Thus, the total number of sensors will be 6 to 168 if adding two types of sensors together. Fig. 3(a) shows the measurement accuracy changes versus the total numbers of strain sensors. As the temperature increases, an accurate measurement will require more sensors when compared to lower temperatures. For all four different temperature environments, the measurement accuracy changes significantly between 3 and 21 sensors.

To investigate the influence of the total numbers of sensors on the measurement accuracy, another analysis was performed by changing the total numbers of strain sensors from 1 to 21 sensors with increments of 1 as shown in Fig. 3(b) based on the same assumption used in Fig. 3(a). If the required measurement accuracy is 90% for all four-temperature environments (fire environment with temperature up to 1,292 °F), ten strain sensors and ten temperature sensors are needed, resulting in twenty sensors on the column for an adequate measurement accuracy. If a measurement accuracy of 80% is acceptable for all four-temperature environments, three strain sensors and three temperature sensors will be adequate, resulting in a total number of six sensors on the column of interest. A 10% of measurement accuracy could trade off 2/3 of the total numbers of sensors required for the system.

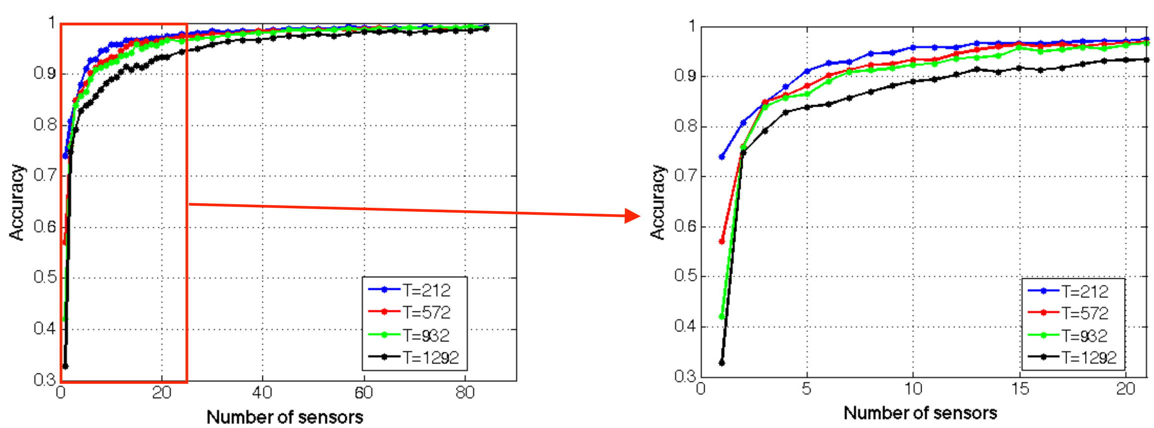

(a) 3~84 strain sensors with an interval of 3 sensors (b) 1~21 strain sensors with an interval of one sensor

Fig. 3 Measurement accuracy versus number of strain sensors for various temperatures

With the optimized number of sensors, the developed GA also delivers the optimized sensor locations. Table 1 shows the optimized sensor locations for the three cases with measurement accuracy of

84.3%, 92.2%, and 95.4% at heating temperature of 212°F. The total numbers of strain sensors ranging from 3 to 9 sensors. With the assumption that at each strain sensor location, there is one temperature sensor, the total number of the two types of sensors ranges from 6 to 18. The sensor layout shows the arrangement of sensors based on their location. A total number of 84 locations were considered with one inch (2.54cm) between each location. In Table 1, a "0" denotes that there is no sensor at that particular location, and a "2" denotes both a temperature and strain sensor being present at that location. For the case of three strain sensors, it can be seen that all the three sensors were located inside the higher temperature range to have a better prediction of the structural behavior of the single-beam frame in fire environments.

Table 1 Sensor layout for 3, 6, and 9 strain sensors for T=212°F

Number of strain sensors	Sensor layout
3	000000000000000000000000000000000000000000000000000000000 000000000000000000000000000000000000000000000000000002000 20000020000000000000000000000000000000000000000000000000
6	020002000000000000000000000000000000000000000000000000000 000000000000000000000000000000002002000000000000000000000 00000000200000000000000200000000000000000000000000000000
9	000000020000000000000000000000000020000000000000000020000 000002000000000000000000000000000000000000200000000000000 00000002020000200000000020000000000000000000000000000000

To validate the developed GA for the sensor placement optimization, the convergence of the genetic algorithm was also investigated as shown in Fig. 4 for three strain sensors at the temperature of 212 °F. The fitness function of the measurement accuracy stabilizes to the optimum value of 84.3% after 2,469 iterations. The maximum iteration was set as 5,000, which is sufficient to provide accurate optimization analysis. The algorithm converged at 2,500 iterations.

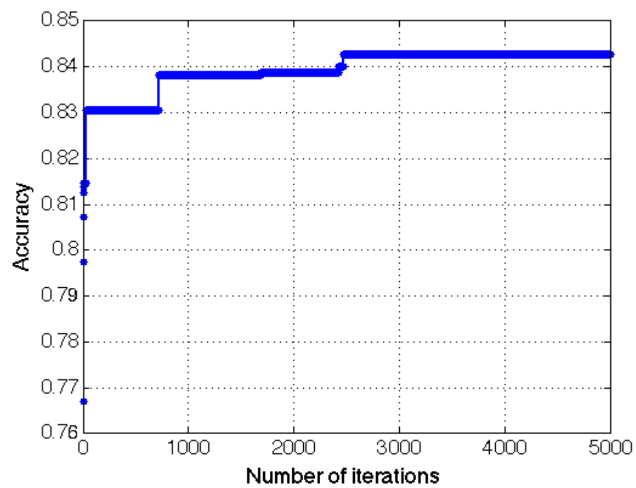

Fig. 4 Number of iterations for GA optimization of 3 strain sensors for T=212°F

3.4 Sensitivity on Sensor Types

The analysis in Section 3.2 is based on the assumption that at each sensor location, we have an equal number of strain and temperature sensors. However, in practical applications, we may have varying sensor types at each sensor location. In this section, the sensitivity on different number of sensors in each sensor type was studied. A case study of a 1/3 ratio of temperature to strain sensors was analyzed based on the assumption that the temperature sensors will be located at one of the strain sensor locations. Fig. 5 shows the measurement accuracy versus the total numbers of temperature sensors in the case of a 1/3 temperature/strain ratio from 1 to 21 sensors with increments of one based on the same assumption at each sensor location. Fig. 5 indicates that with two temperature sensors and six strain sensors, the measurement accuracy for all four-temperature environments will be higher than 80%, resulting in a total number of eight sensors required. If the requirement of a measurement accuracy is 90% for a temperature environment up to 1,292 °F, it will need 9 temperature sensors and 27 strain sensors totaling to 36 sensors. For an unequal number of sensors for different type of sensors, a 10% of measurement accuracy could trade off as high as 3/4 of the total cost for the system. By comparing Fig. 4(b) and Fig. 5, it can be seen that two temperature sensors and six strain sensors show similar measurement accuracy with three temperature sensors and three strain sensors. If a temperature sensor has a cost of three times higher than the strain sensors, the two cases will yield the same fitness value.

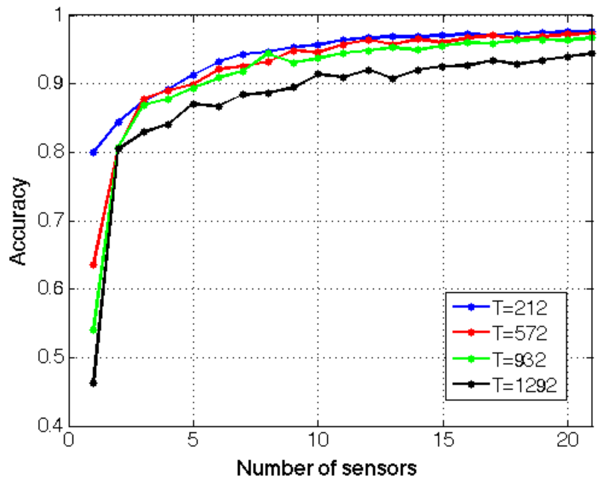

Fig. 5 Measurement accuracy vs number of temperature sensors for various temperatures with unequal numbers of strain and temperature sensors

The optimized sensor locations for the unequal numbers of different types of sensors can also be obtained through the developed GA. Table 2 shows the optimized sensor locations with the numbers of temperature sensors ranging from one to three sensors at 212 °F. In the sensor layout, a "0" denotes no sensor at that location, a "1" denotes only a strain sensor at that location, and a "2" denotes both a temperature and strain sensor being present at that location. Table 2 demonstrates that if only one temperature sensor is applied in this case study, the temperature sensor will be placed at the middle of the temperature-loading zone.

Table 2 Sensor layout for the unequal case at T=212°F

Number of temperature sensors	Sensor layout
1	000010000000000000000000000000000000000000000000000000000 000000000000000002000000000000000000000000000000000000000 00000000000000000000000000000000000010000000000000000000
2	001000000000000010000001000000000000000000000000000001000 000000000000000000000000000000000000000000000000000000002 00000000000000000000020000000000000000000000000000000000
3	000000100000001000000000000000000000000001000000000000000 000000000000010000000000000000000000000000000000000000000 00000002100200002000000000000100000000000000000000000000

4. Experimental Validation and Discussions

Section 3 demonstrated that with a known required measurement accuracy, the total number of sensors, the types of sensors to be applied, and the locations of the associated sensors can be optimized using the developed GA. To validate the effectiveness of the developed GA method for sensor placement optimization of SHM system in harsh environments, laboratory experiments were performed based on the case study in Section 3 as shown in Fig. 6. The material and the size of the steel frame were built the same as described in Section 3.1. A tube furnace made by Thermo Scientific (Model: Lindberg/Blue M) was used to provide a temperature change environment for validation. It had three temperature zones that can be programmed and operated independently, which were programmed to have the same temperature increase profile in this validation test. The temperature in the furnace was increased at a rate of 18 °F/min (10 °C/min) from 72 °F (room temperature, 22 °C) to 1,292°F (700 °C) by an interval of 180 °F (100 °C). At each temperature level, the test paused for 10 minutes to ensure that the temperature distribution is stable both inside and outside the furnace. Vertical load was applied on the top beam by the displacement-controlled actuator of 4.6 kips (20.46 kN) to 10 kips (44.48 kN).

Fig. 6 Laboratory experimental setup

4.1 Sensor Layout from the Developed Algorithm

To validate the effectiveness of the developed GA for sensor placement optimization, a comprehensive sensing network was applied on the steel frame at the identified locations based on the analysis in Section 3.4 for two temperature sensors and six strain sensors as shown in Fig. 7 for the detailed locations of the installed sensors. This validation test used sensors developed in reference to [35] for simultaneous high temperature and large strain measurements. The temperature sensors used long period fiber grating (LPFG) and the strain sensors used movable extrinsic Fabry-Perot interferometer (EFPI) large strain sensors [35]. Ceramic adhesives that can endure high temperatures up to 2,012 °F (1,100 °C) were used to attach optical sensors on the surface of the column flanges.

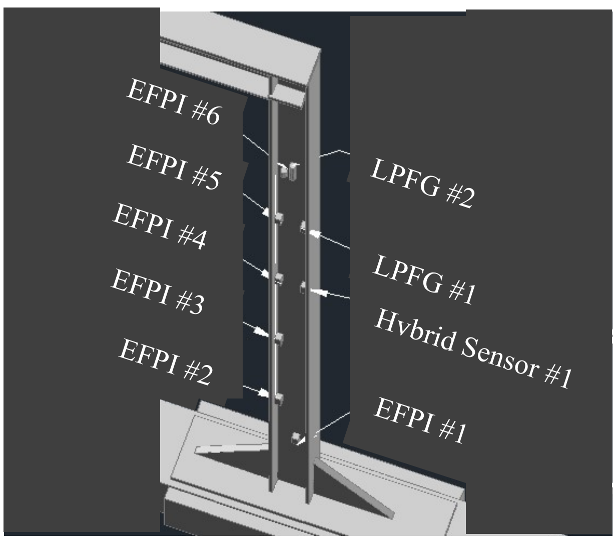

(a) Sensor layout based on developed GA

(b) Test scene with installed sensors

Fig. 7 Sensor layout in the laboratory experiment

4.2 Experimental Results and Discussion

Fig. 8 shows the measured temperature and strains at the installed sensor locations using the location identified by the developed GA. From the measurements, it is clearly seen that the steel frame experienced harsh environment with simultaneous high temperature up to 1,292°F (700 °C) and large deformation up to 8%. Using the measured strains and temperatures, the strain and temperatures at other locations on the column were calculated based on linear interpolation. Fig. 9, therefore, compares the measurement accuracy changes as simulated fire temperature increases from the experiments and that from the theoretic analysis obtained by the algorithm as shown in Section 3.4. At the temperature of 212 °F (100 °C), the measurement accuracy is predicted to be 85% and the actual measurement accuracy from the experiment is 88%. The measurement accuracy at 1,292°F (700 °C) was expected to be 80% from the training, and the measured accuracy through experiments is 76%. A variance less than 5% between the theoretical and the experimental analysis indicates a very effective sensor placement optimization using the developed GA.

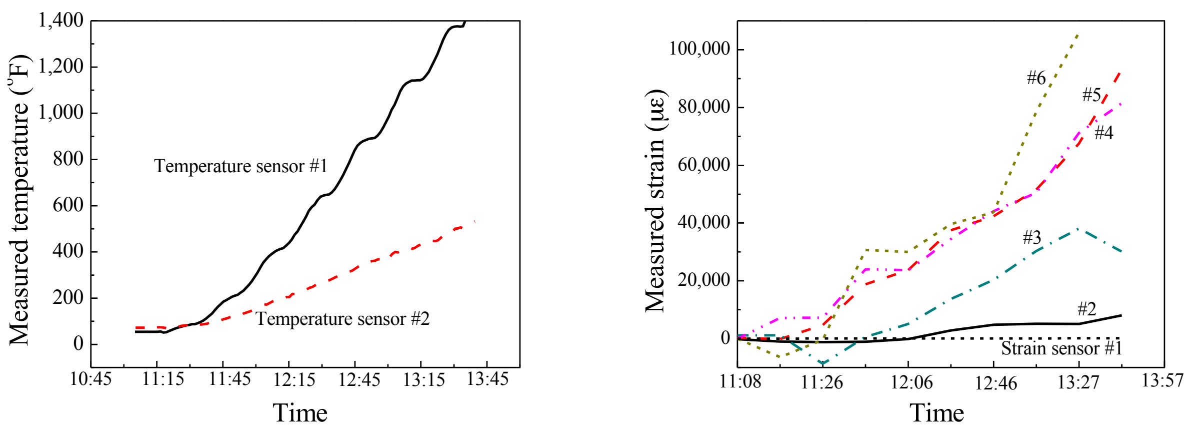

(a) Measured temperatures (b) Measured strains

Fig. 8 Measured temperature and strain as furnace temperature increases

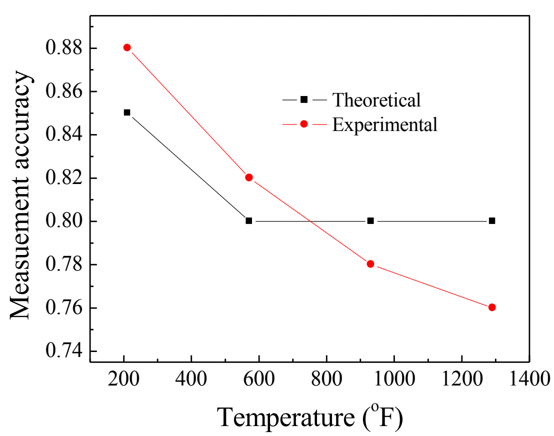

Fig. 9 Comparison between theoretic and experimental analysis

5. Conclusions and Future Work

This paper outlines an effective approach for sensor placement optimization with consideration of the tradeoff between measurement accuracy and cost of the system. The authors conducted a theoretic and numerical analysis to develop the algorithm followed by laboratory validation experiments. The conclusions of this paper are as follows:

1) In harsh environments, structures will require multiple types of sensors with different cost consideration. A GA developed in this article can optimize the sensor placement for structural health monitoring in harsh environments using a fitness function with considerations of parameters from multiple types of sensors.
2) Numerical simulation for a case study on a single-bay one-story steel frame in fire as harsh environment proved that with a known required measurement accuracy of a SHM system, the total numbers of sensors, the types of sensors to be applied, and the locations of the associated sensors can be optimized using the developed GA. If equal numbers of strain and temperature sensors are placed at one location, a measurement accuracy of 80% to be achieved will need three strain and temperature sensors; and if unequal numbers of strain and temperature sensors (1/3 temperature/strain sensor ratio) are allowed, 80% of measurement accuracy will need two temperature sensors and six strain sensors.
3) The laboratory experiments validated the results of the developed GA for sensor placement optimization of SHM system in harsh environments using the single-bay one-story steel frame case study. The sensors placement layout based on the developed GA with two temperature sensors and six strain sensors yielded a measurement accuracy of 76% in a fire environment of 1,292 °F (700 °C), which is very close to the expected value of 80% obtained by the numerical analysis.

The results of this research provide an effective way to place optimal numbers of sensors with a consideration of both measurement accuracy and cost on the target significant structures in harsh environments such as tall buildings, hospitals, nuclear power plants, etc. The current algorithm is applicable for one-dimension (1-D) problems. Future work will apply this method to multiple dimension problems such as structures in three dimensions (3-D) and include more parameters to be considered such as vibration and moisture if needed.

References

1. Boyd S, Vandenberghe L (2004) Convex optimization. Cambridge university press,

2. Garey MR, Johnson DS (1979) Computers and intractability: a guide to the theory of NP-completeness. 1979. San Francisco, LA: Freeman

3. Bian F, Kempe D, Govindan R Utility based sensor selection. In: Proceedings of the 5th international conference on Information processing in sensor networks, 2006. ACM, pp 11-18

4. Joshi S, Boyd S (2009) Sensor selection via convex optimization. Signal Processing, IEEE Transactions on 57 (2):451-462

5. Kincaid RK, Padula SL (2002) D-optimal designs for sensor and actuator locations. Computers & Operations Research 29 (6):701-713

6. Das A, Kempe D Sensor selection for minimizing worst-case prediction error. In: Information Processing in Sensor Networks, 2008. IPSN'08. International Conference on, 2008. IEEE, pp 97-108

7. Kammer DC (1991) Sensor placement for on-orbit modal identification and correlation of large space structures. Journal of Guidance, Control, and Dynamics 14 (2):251-259

8. Udwadia FE (1994) Methodology for optimum sensor locations for parameter identification in dynamic systems. Journal of Engineering Mechanics 120 (2):368-390

9. Kirkegaard PH, Brincker R (1994) On the optimal location of sensors for parametric identification of linear structural systems. Mechanical Systems and Signal Processing 8 (6):639-647

10. Penny J, Friswell M, Garvey S (1994) Automatic choice of measurement locations for dynamic testing. AIAA journal 32 (2):407-414

11. Cobb RG, Liebst B (1996) Sensor location prioritization and structural damage localization using minimal sensor information. AIAA J 35 (2):369-374

12. Reynier M, Abou-Kandil H (1999) Sensors location for updating problems. Mechanical systems and signal processing 13 (2):297-314

13. Shi Z, Law S, Zhang L (2000) Optimum sensor placement for structuraldamage detection. Journal of Engineering Mechanics 126 (11):1173-1179

14. Heredia-Zavoni E, Esteva L (1998) Optimal instrumentation of uncertain structural systems subject to earthquake ground motions. Earthquake engineering & structural dynamics 27 (4):343-362

15. Kammer DC, Tinker ML (2004) Optimal placement of triaxial accelerometers for modal vibration tests. Mechanical systems and signal processing 18 (1):29-41

16. Kammer DC (2005) Sensor set expansion for modal vibration testing. Mechanical systems and signal processing 19 (4):700-713

17. Papadimitriou C, Beck JL, Au S-K (2000) Entropy-based optimal sensor location for structural model updating. Journal of Vibration and Control 6 (5):781-800

18. Papadimitriou C (2005) Pareto optimal sensor locations for structural identification. Computer Methods in Applied Mechanics and Engineering 194 (12):1655-1673

19. Yuen K-V, Katafygiotis LS, Papadimitriou C, Mickleborough NC (2001) Optimal sensor placement methodology for identification with unmeasured excitation. Journal of dynamic systems, measurement, and control 123 (4):677-686

20. Rao ARM, Anandakumar G (2007) Optimal placement of sensors for structural system identification and health monitoring using a hybrid swarm intelligence technique. Smart materials and Structures 16 (6):2658

21. Srinivas M, Patnaik LM (1994) Genetic algorithms: A survey. Computer 27 (6):17-26

22. Han J-H, Lee I (1999) Optimal placement of piezoelectric sensors and actuators for vibration control of a composite plate using genetic algorithms. Smart Materials and Structures 8 (2):257

23. Guo H, Zhang L, Zhang L, Zhou J (2004) Optimal placement of sensors for structural health monitoring using improved genetic algorithms. Smart Materials and Structures 13 (3):528

24. Yi T-H, Li H-N, Gu M (2011) Optimal sensor placement for health monitoring of high-rise structure based on genetic algorithm. Mathematical Problems in Engineering, 2011: 395101-12

25. Huang M, Li J, Zhu H (2009) Optimal sensor layout for bridge health monitoring based on dual-structure coding genetic algorithm. In: 2009 International Conference on IEEE Computational Intelligence and Software Engineering, pp 1-4

26. Cha Y-J, Agrawal AK, Kim Y, Raich AM (2012) Multi-objective genetic algorithms for cost-effective distributions of actuators and sensors in large structures. Expert Systems with Applications 39 (9):7822-7833

27. Yi T-H, Li H-N, Gu M (2011) Optimal sensor placement for structural health monitoring based on multiple optimization strategies. The Structural Design of Tall and Special Buildings, 20(7): 881-900

28. Yi T-H, Li H-N (2012) Methodology developments in sensor placement for health monitoring of civil infrastructures. International Journal of Distributed Sensor Networks, 2012: 612726

29. Yi T-H, Li H-N, Wang X, (2013) Multi-dimensional sensor placement optimization for Canton Tower focusing on application demands. Smart Structures and Systems, an International Journal, 12(3-4): 235-250

30. Yi T-H, Li H-N, Zhang X-D, (2012) Sensor placement on Canton Tower for health monitoring using asynchronous-climb monkey algorithm. Smart Materials and Structures, 21(12):125023

31. Zhou G-D, Yi T-H, Zhang H, and Li H-N (2015) Optimal sensor placement under uncertainties using a nondirective movement glowworm swarm optimization algorithm. Smart Structures and Systems, an International Journal, 16(2): 243-262

32. Yi T-H, Li H-N, Zhang X-D (2015) Health monitoring sensor placement optimization for Canton Tower using immune monkey algorithm. Structural Control and Health Monitoring, 22(1): 123-138

33. Eiben A, Smith J (2008) Introduction to evolutionary computing (natural computing series).

34. Holland JH (1992) Adaptation in natural and artificial systems: an introductory analysis with applications to biology, control, and artificial intelligence. MIT press,

35. Huang Y, Fang X, Bevans WJ, Zhou Z, Xiao H, Chen G (2013) Large-strain optical fiber sensing and real-time FEM updating of steel structures under the high temperature effect. Smart Materials and Structures 22 (1):015016

36. Abaqus/Standard user's manual 6.9.1 (2009), Hibbit, Karlsson & Sorensen, Inc., Pawtucket, Rhode Island, US.